

# $^1\text{H}$ and $^{19}\text{F}$ NMR Studies on Molecular Motions in Two Solid Phases of t-Butylammonium Tetrafluoroborate

Hiroyuki Ishida

Department of Chemistry, Faculty of Science, Okayama University, Okayama 700-8530, Japan

Z. Naturforsch. **53 a**, 796–800 (1998); received May 30, 1998

Differential thermal analysis (DTA), differential scanning calorimetry (DSC), and the temperature dependence of the spin-lattice relaxation time ( $T_1$ ) and the second moment ( $M_2$ ) of  $^1\text{H}$  and  $^{19}\text{F}$  NMR were studied in  $(\text{CH}_3)_3\text{CNH}_3\text{BF}_4$  and  $(\text{CH}_3)_3\text{CND}_3\text{BF}_4$ . DTA and DSC revealed a solid-solid phase transition at 219 K for  $(\text{CH}_3)_3\text{CNH}_3\text{BF}_4$  and at 221 K for  $(\text{CH}_3)_3\text{CND}_3\text{BF}_4$ . The motions of cations and anions in the two solid phases were studied by  $T_1$  and  $M_2$  experiments. The motional modes of the ions and their motional parameters were determined.

**Key words:** Molecular motion; Phase transition; Nuclear magnetic resonance.

## Introduction

In previous papers we have studied  $(\text{CH}_3)_3\text{CNH}_3\text{NO}_3$  [1] and  $(\text{CH}_3)_3\text{CNH}_3\text{ClO}_4$  [2] by  $^1\text{H}$  NMR and thermal measurements. The nitrate was found to have seven solid phases (including three metastable phases) between 80 K and the melting point (418 K). The perchlorate has four solid phases (including a metastable phase) between 80 K and the melting point (414 K). We discussed the molecular motions of the cation in each phase and the relation between the motions and the polymorphic phase transitions.

Since a  $\text{BF}_4^-$  ion is expected to be able to move easily in crystals because of its highly symmetric shape and its size similarity to  $\text{ClO}_4^-$ , and since  $^{19}\text{F}$  NMR can be measured as easily as  $^1\text{H}$  NMR, t-butylammonium tetrafluoroborate seems to be an interesting candidate for studying the motions of both cation and anion, and the phase transition triggered by the molecular motion. In the present study,  $^1\text{H}$  and  $^{19}\text{F}$  NMR, differential thermal analysis (DTA), and differential scanning calorimetry (DSC) have been performed on  $(\text{CH}_3)_3\text{CNH}_3\text{BF}_4$  and its partially deuterated analog,  $(\text{CH}_3)_3\text{CND}_3\text{BF}_4$ , to characterize the molecular motions of both cation and anion and to investigate possible phase transitions.

## Experimental

$(\text{CH}_3)_3\text{CNH}_3\text{BF}_4$  was prepared by neutralizing t-butylamine with tetrafluoroboric acid. The obtained crystals were recrystallized twice from isopropyl alcohol. Found: C, 29.80; H, 7.45; N, 8.61%. Calcd for  $(\text{CH}_3)_3\text{CNH}_3\text{BF}_4$ : C, 29.85; H, 7.52; N, 8.70%.  $(\text{CH}_3)_3\text{CND}_3\text{BF}_4$  was prepared from purified  $(\text{CH}_3)_3\text{CNH}_3\text{BF}_4$  by three times repeated crystallization from  $\text{D}_2\text{O}$  (99.8 D%). Because of the hygroscopicity of the purified crystals, they were handled in a dry bag and dried under a vacuum (ca.  $10^{-1}$  Pa) at room temperature for 5 h and then at 70 °C for 5 h before the NMR, DTA, and DSC measurements. The phase transition temperatures and the corresponding enthalpy changes were determined on a home-made DTA apparatus [3] and a Perkin-Elmer DSC7, respectively, at 100 to 410 K. The second moment of the  $^1\text{H}$  and  $^{19}\text{F}$  NMR linewidths (abbreviated to  $M_{2\text{H}}$  and  $M_{2\text{F}}$ , respectively) was determined by use of a JEOL JNM-MW-40S spectrometer. The spin-lattice relaxation times of  $^1\text{H}$  and  $^{19}\text{F}$  NMR (abbreviated to  $T_{1\text{H}}$  and  $T_{1\text{F}}$ , respectively) were measured using a pulsed NMR spectrometer [4] with the  $180^\circ - t - 90^\circ$  pulse sequence.

## Results and Discussion

### DTA and DSC

A solid-solid phase transition and the melting point were located at  $219 \pm 1$  and  $404 \pm 1$  K, respectively,

Reprint requests to Prof. Dr. H. Ishida;  
Fax: +81 86 251 8497.

0932-0784 / 98 / 0900-0796 \$ 06.00 © Verlag der Zeitschrift für Naturforschung, Tübingen · www.znaturforsch.com



Dieses Werk wurde im Jahr 2013 vom Verlag Zeitschrift für Naturforschung in Zusammenarbeit mit der Max-Planck-Gesellschaft zur Förderung der Wissenschaften e.V. digitalisiert und unter folgender Lizenz veröffentlicht: Creative Commons Namensnennung-Keine Bearbeitung 3.0 Deutschland Lizenz.

Zum 01.01.2015 ist eine Anpassung der Lizenzbedingungen (Entfall der Creative Commons Lizenzbedingung „Keine Bearbeitung“) beabsichtigt, um eine Nachnutzung auch im Rahmen zukünftiger wissenschaftlicher Nutzungsformen zu ermöglichen.

This work has been digitalized and published in 2013 by Verlag Zeitschrift für Naturforschung in cooperation with the Max Planck Society for the Advancement of Science under a Creative Commons Attribution-NoDerivs 3.0 Germany License.

On 01.01.2015 it is planned to change the License Conditions (the removal of the Creative Commons License condition “no derivative works”). This is to allow reuse in the area of future scientific usage.

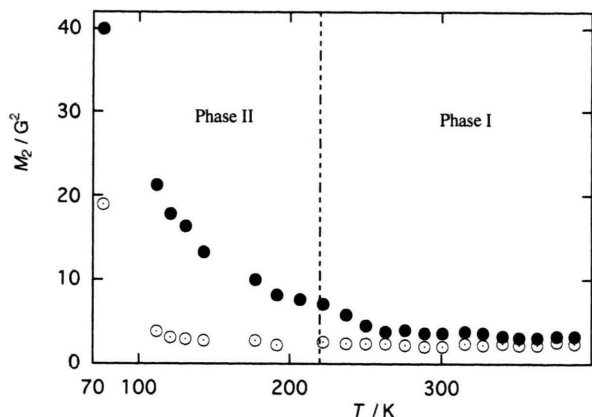


Fig. 1. Temperature dependence of the  $^1\text{H}$  (●) and  $^{19}\text{F}$  (○) NMR second moment ( $M_2$ ) observed in  $(\text{CH}_3)_3\text{CNH}_3\text{BF}_4$ . The broken line shows the phase transition temperature determined by DTA.

for  $(\text{CH}_3)_3\text{CNH}_3\text{BF}_4$  by DTA. Since the heat anomaly at the solid-solid phase transition showed a long tail on the low temperature side on both heating and cooling runs, we have assigned the peak temperature to the transition temperature. The revealed solid phases are designated in the order of decreasing temperature as Phases I and II. The enthalpy changes at transition and fusion determined by DSC were  $0.49 \pm 0.05$  and  $12.6 \pm 0.5 \text{ kJ mol}^{-1}$ , respectively; thus the associated entropy changes were calculated to be  $2.2 \pm 0.2$  and  $31 \pm 1 \text{ J K}^{-1} \text{ mol}^{-1}$ , in the same order. The solid-solid transition temperature determined for  $(\text{CH}_3)_3\text{CND}_3\text{BF}_4$  by DTA was  $221 \pm 1 \text{ K}$ .

#### Second Moment ( $M_2$ ) of $^1\text{H}$ and $^{19}\text{F}$ NMR Linewidths

The temperature dependences of  $M_{2\text{H}}$  and  $M_{2\text{F}}$  observed for  $(\text{CH}_3)_3\text{CNH}_3\text{BF}_4$  are shown in Figure 1. The  $M_{2\text{H}}$  and  $M_{2\text{F}}$  values at 77 K are  $40 \pm 0.5$  and  $19 \pm 0.3 \text{ G}^2$  ( $1 \text{ G} = 1 \times 10^{-4} \text{ T}$ ), respectively. These values imply that both cation and anion are rigid at 77 K because the observed  $M_{2\text{H}}$  and  $M_{2\text{F}}$  values are much larger than  $25.7 \text{ G}^2$  [2] and  $14.5 \text{ G}^2$  [5], respectively, as calculated for the rigid states of the isolated cation and anion. The differences between the observed and calculated values are attributable to intermolecular contributions. With increasing temperature,  $M_{2\text{F}}$  decreased rapidly and a constant value of  $2.3 \pm 0.2 \text{ G}^2$  was obtained above 120 K. This value can be attributed to the isotropic reorientation of the  $\text{BF}_4^-$  ion, referring to the  $M_{2\text{F}}$  results obtained in

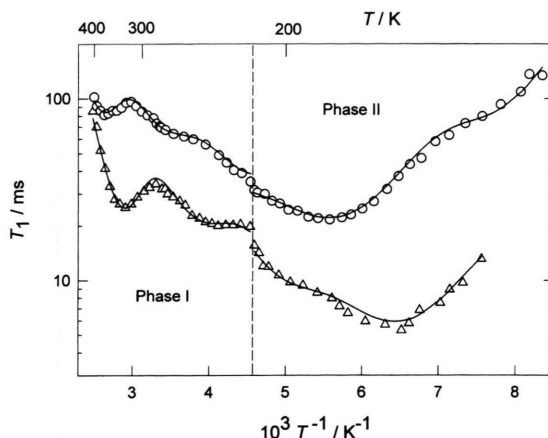


Fig. 2. Temperature dependence of  $^1\text{H}$  NMR spin-lattice relaxation time ( $T_{1\text{H}}$ ) observed at 8.5 ( $\Delta$ ) and 32 (○) MHz in  $(\text{CH}_3)_3\text{CNH}_3\text{BF}_4$ . The solid lines indicate the best-fit theoretical values; the broken line shows the phase transition temperature determined by DTA.

$\text{NH}_4\text{BF}_4$  [5, 6], in which an  $M_{2\text{F}}$  of 2.5–2.8  $\text{G}^2$  was reported for the anionic motion.  $M_{2\text{H}}$  decreased, on the other hand, in three steps and reached a constant value of  $3.2 \pm 0.2 \text{ G}^2$  above 340 K. This value agrees fairly well with the  $3.8 \text{ G}^2$  calculated for the cation which performs the  $\text{C}_3'$  reorientation of the t-butyl group about the C–N bond axis together with the  $\text{C}_3$  reorientations of the  $\text{CH}_3$  and  $\text{NH}_3^+$  groups about the C–C and C–N bond axes, respectively [2]. The result that the observed  $M_{2\text{H}}$  value is smaller than the calculated  $M_{2\text{H}}$  value is explainable in terms of the contribution to  $M_{2\text{H}}$  from the large-amplitude librations of the cation about its C–C and/or C–N bond axes as discussed in previous papers [2, 7–9].

#### Spin-lattice Relaxation Time ( $T_{1\text{H}}$ ) of $^1\text{H}$ NMR

The temperature dependence of  $T_{1\text{H}}$  observed for  $(\text{CH}_3)_3\text{CNH}_3\text{BF}_4$  at Larmor frequencies of 8.5 and 32 MHz is shown in Figure 2.  $T_{1\text{H}}$  at 8.5 MHz showed three minima at 155, 245 and 345 K, and a shoulder around 200 K. No marked change in  $T_{1\text{H}}$  was observed at the transition point of 219 K. The temperature dependences of  $T_{1\text{H}}$  at 8.5 and 32 MHz in  $(\text{CH}_3)_3\text{CND}_3\text{BF}_4$  are shown in Figure 3.  $T_{1\text{H}}$  at 8.5 MHz shows two minima at 155 and 345 K, and a shoulder around 200 K. Among the three kinds of cationic motions observed, i. e., the  $\text{CH}_3$ ,  $\text{NH}_3^+$ , and t-butyl groups reorientations, the  $\text{NH}_3^+$  group motion was found to correspond to the  $T_{1\text{H}}$  minimum at

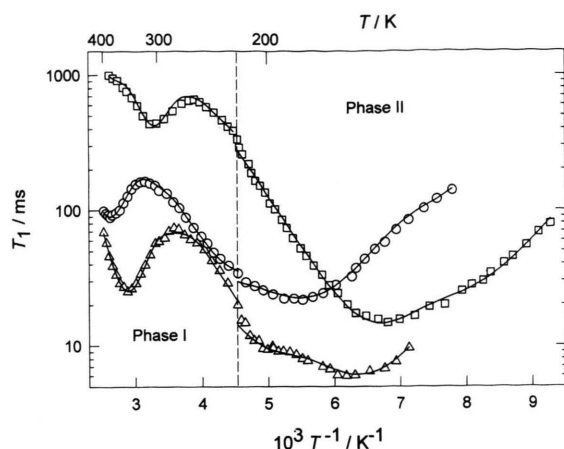


Fig. 3. Temperature dependence of spin-lattice relaxation time for  $^1\text{H}$  ( $T_{1\text{H}}$ ) and  $^{19}\text{F}$  ( $T_{1\text{F}}$ ) observed in  $(\text{CH}_3)_3\text{CND}_3\text{BF}_4$ .  $T_{1\text{H}}$  ( $\Delta$ ) observed at 8.5 MHz;  $T_{1\text{H}}$  ( $\circ$ ) at 32 MHz;  $T_{1\text{F}}$  ( $\square$ ) at 30.1 MHz. The solid lines indicate the best-fit theoretical values; the broken line shows the phase transition temperature determined by DTA.

245 K in  $(\text{CH}_3)_3\text{CNH}_3\text{BF}_4$ , comparing the  $T_{1\text{H}}$  data in  $(\text{CH}_3)_3\text{CNH}_3\text{BF}_4$  with those in  $(\text{CH}_3)_3\text{CND}_3\text{BF}_4$ . The  $T_{1\text{H}}$  minimum and the shoulder in Phase II can, therefore, be attributed to the  $\text{CH}_3$  group reorientation and the  $T_1$  minimum at 345 K in Phase I to the t-butyl group motion because the  $\text{CH}_3$  group motion is expected to occur more easily, i.e., at lower temperatures than the t-butyl group motion.

The broad and asymmetric  $T_{1\text{H}}$  minimum in Phase II, assignable to the  $\text{CH}_3$  group motion, can be explained in terms of the existence of crystallographic non-equivalent  $\text{CH}_3$  groups. Assuming two kinds of  $\text{CH}_3$  groups in this phase,  $T_{1\text{H}}$  can be expressed by considering the  $^1\text{H}$ - $^1\text{H}$  and  $^1\text{H}$ - $^{19}\text{F}$  magnetic dipolar interactions [10 - 12],

$$\frac{1}{T_{1\text{H}}} = C_{\text{HH}(1)}g(\omega_{\text{H}}, \tau_{\text{H}(1)}) + C_{\text{HH}(2)}g(\omega_{\text{H}}, \tau_{\text{H}(2)}) + C_{\text{HF}(1)}g(\omega_{\text{HF}}, \tau_{\text{H}(1)}) + C_{\text{HF}(2)}g(\omega_{\text{HF}}, \tau_{\text{H}(2)}); \quad (1)$$

$$g(\omega_{\text{H}}, \tau_{\text{H}(i)}) = \frac{\tau_{\text{H}(i)}}{1 + \omega_{\text{H}}^2 \tau_{\text{H}(i)}^2} + \frac{4\tau_{\text{H}(i)}}{1 + 4\omega_{\text{H}}^2 \tau_{\text{H}(i)}^2}, \quad (2)$$

$$g(\omega_{\text{HF}}, \tau_{\text{H}(i)}) = \frac{\tau_{\text{H}(i)}}{1 + (\omega_{\text{H}} - \omega_{\text{F}})^2 \tau_{\text{H}(i)}^2} + \frac{3\tau_{\text{H}(i)}}{1 + \omega_{\text{H}}^2 \tau_{\text{H}(i)}^2} + \frac{6\tau_{\text{H}(i)}}{1 + (\omega_{\text{H}} + \omega_{\text{F}})^2 \tau_{\text{H}(i)}^2} \quad (3)$$

( $i = 1, 2$ ).

Table 1. Activation energies  $E_a$ , correlation times  $\tau_0$  at the limit of infinite temperature, and motional constants evaluated for anionic and cationic motions in Phases I and II of  $(\text{CH}_3)_3\text{CNH}_3\text{BF}_4$  and  $(\text{CH}_3)_3\text{CND}_3\text{BF}_4$  by measurement of  $^1\text{H}$  and  $^{19}\text{F}$  NMR spin-lattice relaxation time.

$E_a / \text{kJ mol}^{-1}$	$\tau_0 / 10^{-13} \text{ s}$	$C / 10^8 \text{ s}^{-2}$	Reorienting group
$(\text{CH}_3)_3\text{CNH}_3\text{BF}_4$ , Phase I:			
40*	0.11*	$12.3 \pm 0.1$ ( $C'_{\text{HH}}$ ) $0.25 \pm 0.02$ ( $C'_{\text{HF}}$ )	t-butyl
16*	4*	$34 \pm 1$ ( $C_{\text{HH}}$ )	$\text{CH}_3$
$24 \pm 1$	$1.4 \pm 0.1$	$11.5 \pm 0.5$ ( $C''_{\text{HH}}$ ) $0.30 \pm 0.05$ ( $C''_{\text{HF}}$ )	$\text{NH}_3^+$
$(\text{CH}_3)_3\text{CNH}_3\text{BF}_4$ , Phase II:			
$13 \pm 1$	$4.9 \pm 0.5$	$50 \pm 2$ ( $C_{\text{HH}(1)}$ ) $2.0 \pm 0.1$ ( $C_{\text{HF}(1)}$ )	$\text{CH}_3(1)$
$16 \pm 1$	$7.5 \pm 0.5$	$23 \pm 1$ ( $C_{\text{HH}(2)}$ ) $0.9 \pm 0.1$ ( $C_{\text{HF}(2)}$ )	$\text{CH}_3(2)$
$(\text{CH}_3)_3\text{CND}_3\text{BF}_4$ , Phase I:			
$40 \pm 2$	$0.11 \pm 0.3$	$13.3 \pm 0.1$ ( $C_{\text{HH}}$ ) $0.25 \pm 0.02$ ( $C_{\text{HF}}$ )	t-butyl
$16 \pm 2$	$4 \pm 1$	$40 \pm 1$ ( $C_{\text{HH}}$ )	$\text{CH}_3$
$10 \pm 1$	—	—	$\text{BF}_4^-$
$(\text{CH}_3)_3\text{CND}_3\text{BF}_4$ , Phase II:			
$13 \pm 1$	$5.2 \pm 0.5$	$53 \pm 1$ ( $C_{\text{HH}(1)}$ ) $1.0 \pm 0.2$ ( $C_{\text{HF}(1)}$ )	$\text{CH}_3(1)$
$16 \pm 1$	$8.0 \pm 0.5$	$25 \pm 1$ ( $C_{\text{HH}(2)}$ ) $0.5 \pm 0.1$ ( $C_{\text{HF}(2)}$ )	$\text{CH}_3(2)$
$10.3 \pm 0.4$	$3 \pm 1$	$34 \pm 3$ ( $C_{\text{FF}(1)}$ )	$\text{BF}_4(1)^-$
$17.2 \pm 0.8$	$0.07 \pm 0.04$	$34 \pm 3$ ( $C_{\text{FF}(2)}$ )	$\text{BF}_4(2)^-$

\* Values obtained in Phase I of  $(\text{CH}_3)_3\text{CND}_3\text{BF}_4$ .

Here  $\tau_{\text{H}(1)}$  and  $\tau_{\text{H}(2)}$  denote the reorientational correlation times of the two kinds of  $\text{CH}_3$  groups giving the  $T_{1\text{H}}$  minimum at the low and high temperatures, respectively;  $\omega_{\text{H}}$  and  $\omega_{\text{F}}$  are the  $^1\text{H}$  and  $^{19}\text{F}$  Larmor frequencies.  $C_{\text{HH}(i)}$  and  $C_{\text{FH}(i)}$  stand for the motional constants related to the reduction of  $M_{2\text{H}}$  through the  $^1\text{H}$ - $^1\text{H}$  and  $^1\text{H}$ - $^{19}\text{F}$  interactions, respectively, due to the  $i$ -th  $\text{CH}_3$  group motion. Equations (1) - (3) were fitted to the  $T_{1\text{H}}$  observed in Phase II of  $(\text{CH}_3)_3\text{CNH}_3\text{BF}_4$  and  $(\text{CH}_3)_3\text{CND}_3\text{BF}_4$ . In the calculations, we assumed an Arrhenius-type relationship between  $\tau_{\text{H}(i)}$  and the activation energy ( $E_{a(i)}$ ) ( $i = 1, 2$ ) of the motional process expressed as

$$\tau_{\text{H}(i)} = \tau_{0(i)} \exp(E_{a(i)}/RT), \quad (4)$$

where  $\tau_{0(i)}$  is the correlation time at the limit of infinite temperature. The optimum values of  $C_{\text{HH}(i)}$ ,  $C_{\text{HF}(i)}$ ,  $\tau_{0(i)}$ , and  $E_{a(i)}$  are shown in Table 1 and the fitted curves are shown in Figs. 2 and 3. We obtained

$C_{\text{HH}(1)} = 50 \times 10^8$  and  $C_{\text{HH}(2)} = 23 \times 10^8 \text{ s}^{-2}$  for  $(\text{CH}_3)_3\text{CNH}_3\text{BF}_4$  and  $C_{\text{HH}(1)} = 53 \times 10^8$  and  $C_{\text{HH}(2)} = 25 \times 10^8 \text{ s}^{-2}$  for  $(\text{CH}_3)_3\text{CND}_3\text{BF}_4$ , implying that the nonequivalent  $\text{CH}_3$  groups can be classified into two groups with an abundance ratio of 2:1. The activation energies of 13 and 16  $\text{kJ mol}^{-1}$  obtained for the  $\text{CH}_3$  reorientations are comparable to the potential barrier of 17.21  $\text{kJ mol}^{-1}$  for the internal rotation of the  $\text{CH}_3$  group in an isolated t-butylammonium ion calculated by ab initio MO [13], when one takes into account the zero-point energy. The reorientation of the  $\text{CH}_3$  group in this phase is, therefore, expected to be mostly hindered by the intra-cationic potential barrier, and the intermolecular hindrance to the reorientation is considered to be small.

The  $T_{1\text{H}}$  minima at 8.5 and 32 MHz in Phase I of  $(\text{CH}_3)_3\text{CND}_3\text{BF}_4$  are attributed to the t-butyl group reorientation, as mentioned above. The  $T_{1\text{H}}$  increase with temperature in the low-temperature range of Phase I is attributable to the  $\text{CH}_3$  group motion. Since the correlation time ( $\tau_{\text{H}}$ ) for the  $\text{CH}_3$  group motion is considered to be much shorter than that ( $\tau'_{\text{H}}$ ) for the t-butyl group, as predicted from the  $T_{1\text{H}}$  results in Phase II,  $T_{1\text{H}}$  in Phase I can be approximately expressed [10–12, 14] by considering  $^1\text{H}$ - $^1\text{H}$  and  $^1\text{H}$ - $^{19}\text{F}$  dipolar interactions, as

$$\frac{1}{T_{1\text{H}}} = C'_{\text{HH}}g(\omega_{\text{H}}, \tau'_{\text{H}}) + C'_{\text{HF}}g(\omega_{\text{HF}}, \tau'_{\text{H}}) + C_{\text{HH}}g(\omega_{\text{H}}, \tau_{\text{H}}). \quad (5)$$

Here  $C'_{\text{HH}}$  and  $C'_{\text{HF}}$  are the motional constants related to the t-butyl group motion, and  $C_{\text{HH}}$  is related to the  $\text{CH}_3$  group motion. We assumed a single correlation time for the  $\text{CH}_3$  group motion and ignored the contribution from the  $^1\text{H}$ - $^{19}\text{F}$  interaction caused by the  $\text{CH}_3$  group motion for simplicity. Equation (5) is fitted to the  $T_{1\text{H}}$  data using the Arrhenius-type relationship as given by (4) for these two motions.

The  $T_{1\text{H}}$  data in Phase I of  $(\text{CH}_3)_3\text{CNH}_3\text{BF}_4$  can be explained by the t-butyl,  $\text{NH}_3^+$  and  $\text{CH}_3$  group motions, referring to the  $T_{1\text{H}}$  data of  $(\text{CH}_3)_3\text{CND}_3\text{BF}_4$  and the  $M_{2\text{H}}$  results.  $T_{1\text{H}}$  can, therefore, be expressed as

$$\begin{aligned} \frac{1}{T_{1\text{H}}} = & C'_{\text{HH}}g(\omega_{\text{H}}, \tau'_{\text{H}}) + C'_{\text{HF}}g(\omega_{\text{HF}}, \tau'_{\text{H}}) \\ & + C''_{\text{HH}}g(\omega_{\text{H}}, \tau''_{\text{H}}) \\ & + C''_{\text{HF}}g(\omega_{\text{HF}}, \tau''_{\text{H}}) + C_{\text{HH}}g(\omega_{\text{H}}, \tau_{\text{H}}), \end{aligned} \quad (6)$$

where  $\tau''_{\text{H}}$  is the correlation time of  $\text{NH}_3^+$  reorientation, and  $C''_{\text{HH}}$  and  $C''_{\text{HF}}$  are the motional constants. The motional parameters ( $C''_{\text{HH}}$ ,  $C''_{\text{HF}}$ ,  $E_{\text{a}}$ , and  $\tau''_{\text{OH}}$ ) for the  $\text{NH}_3^+$  motion were evaluated using a fitting calculation with the  $E_{\text{a}}$  and  $\tau_0$  values of the t-butyl and  $\text{CH}_3$  group motions obtained from the  $T_{1\text{H}}$  data in Phase I of  $(\text{CH}_3)_3\text{CND}_3\text{BF}_4$ . The  $E_{\text{a}}$  value of 24  $\text{kJ mol}^{-1}$  obtained for the  $\text{NH}_3^+$  motion is considerably smaller than 38.5–44.2  $\text{kJ mol}^{-1}$  for the same motion in t-butylammonium chloride and bromide [15], in which a strong hydrogen bond  $\text{N-H}\cdots\text{X}$  ( $\text{X} = \text{Cl}, \text{Br}$ ) is expected. The value of 24  $\text{kJ mol}^{-1}$  is, however, much larger than 12.41  $\text{kJ mol}^{-1}$ , the calculated potential barrier for the internal rotation of  $\text{NH}_3^+$  [13]. This implies that the primary origin of the hindering force for the  $\text{NH}_3^+$  reorientation is intermolecular interactions including  $\text{N-H}\cdots\text{F}$  hydrogen bonds.

### Spin-lattice Relaxation Time ( $T_{1\text{F}}$ ) of $^{19}\text{F}$ NMR

The  $T_{1\text{F}}$  data of  $(\text{CH}_3)_3\text{CND}_3\text{BF}_4$  observed at 30.1 MHz are shown in Figure 3. The deep  $T_{1\text{F}}$  minimum of 18 ms around 160 K is assignable to the isotropic rotation of the  $\text{BF}_4^-$  ion based on the above discussion on  $M_{2\text{F}}$ . Since the observed  $T_{1\text{F}}$  yielded an asymmetric  $\log T_{1\text{F}}$  vs.  $T^{-1}$  curve, we can expect that at least two kinds of crystallographically nonequivalent anions exist in Phase II. Here we assume that the  $^{19}\text{F}$  -  $^{19}\text{F}$  and  $^{19}\text{F}$  -  $^{11}\text{B}$  magnetic dipole-dipole interactions are the dominant relaxation processes affecting  $T_{1\text{F}}$  and that two kinds of anion exist with an abundance ratio of 1:1, in which case  $T_{1\text{F}}$  can be expressed approximately as [10–12]

$$\begin{aligned} \frac{1}{T_{1\text{F}}} = & C_{\text{FF}(1)}g(\omega_{\text{F}}, \tau_{\text{F}(1)}) + C_{\text{FB}(1)}g(\omega_{\text{FB}}, \tau_{\text{F}(1)}) \\ & + C_{\text{FF}(2)}g(\omega_{\text{F}}, \tau_{\text{F}(2)}) + C_{\text{FB}(2)}g(\omega_{\text{FB}}, \tau_{\text{F}(2)}); \end{aligned} \quad (7)$$

$$g(\omega_{\text{F}}, \tau_{\text{F}(i)}) = \frac{\tau_{\text{F}(i)}}{1 + \omega_{\text{F}}^2 \tau_{\text{F}(i)}^2} + \frac{4\tau_{\text{F}(i)}}{1 + 4\omega_{\text{F}}^2 \tau_{\text{F}(i)}^2}, \quad (8)$$

$$\begin{aligned} g(\omega_{\text{FB}}, \tau_{\text{F}(i)}) = & \frac{\tau_{\text{F}(i)}}{1 + (\omega_{\text{F}} - \omega_{\text{B}})^2 \tau_{\text{F}(i)}^2} + \frac{3\tau_{\text{F}(i)}}{1 + \omega_{\text{F}}^2 \tau_{\text{F}(i)}^2} \\ & + \frac{6\tau_{\text{F}(i)}}{1 + (\omega_{\text{F}} + \omega_{\text{B}})^2 \tau_{\text{F}(i)}^2} \end{aligned} \quad (9)$$

( $i = 1, 2$ ).



Here  $\tau_{F(i)}$  and  $\omega_B$  are the correlation time of isotropic reorientation of the  $i$ -th anion and the Larmor frequency of  $^{11}\text{B}$ . The motional constants,  $C_{FF(i)}$  and  $C_{FB(i)}$ , are the contributions to  $M_{2F}$  caused by  $^{19}\text{F}$ - $^{19}\text{F}$  and  $^{19}\text{F}$ - $^{11}\text{B}$  interactions, respectively, due to the  $i$ -th anionic motion. Since the intra-anionic interaction is dominant for the  $^{19}\text{F}$ - $^{11}\text{B}$  interaction,  $C_{FB(i)}$  is expressed as [10 - 11]

$$C_{FB(i)} = \frac{1}{4} \gamma_F^2 \gamma_B^2 \hbar^2 r_{FB}^{-6} \quad (10)$$

where  $\gamma_F$ ,  $\gamma_B$ , and  $r_{FB}$  are the gyromagnetic ratios of  $^{19}\text{F}$  and  $^{11}\text{B}$ , and the B-F bond distance, respectively. Assuming an Arrhenius-type relationship given by (4), (7) - (9) were fitted to the observed  $T_{1F}$  values, where the theoretical value,  $C_{FB(1)} = C_{FB(2)} = 15 \times 10^8 \text{ s}^{-2}$  ( $r_{FB} = 1.43 \text{ \AA}$ ) [5], was used. The motional parameters determined are given in Table 1, and the best-fit curves are shown in Figure 3.

The  $T_{1F}$  minimum observed in Phase I is thought to originate from the inter-ionic  $^{19}\text{F}$ - $^1\text{H}$  dipolar interactions modulated by the t-butyl group motion because in Phase I intra-anion  $^{19}\text{F}$ - $^{19}\text{F}$  and  $^{19}\text{F}$ - $^{11}\text{B}$  dipolar interactions are considered to be completely averaged out by the anionic isotropic reorientation whose onset is detected in Phase II.  $T_{1F}$  in Phase I can be stated in terms of  $\tau_H'$  and  $\tau_F$ , the correlation times of the t-butyl group and the anion isotropic reorientation, respectively, as

$$\frac{1}{T_{1F}} = C'_{FH} g(\omega_{FH}, \tau_H') + (5C_{FF} + 10C_{FB})\tau_F. \quad (11)$$

Here a single correlation time  $\tau_F$  which is short enough to satisfy the condition of  $\omega_F\tau_F$ ,  $(\omega_F + \omega_B)\tau_F \ll 1$ , is assumed for the anionic motion. Using the correlation time of t-butyl group obtained from the  $T_{1H}$  data of  $(\text{CH}_3)_3\text{CND}_3\text{BF}_4$ , (11) was fitted to the  $T_{1F}$  data in Phase I. The results are shown in Fig. 3 and Table 1.

## Conclusion

The three kinds of cationic motions (reorientations of the  $\text{CH}_3$  groups about their C-C bond axes, the  $\text{NH}_3^+$  group about its C-N bond axis, and the t-butyl group about the C-N bond axis) and the anionic isotropic reorientation were observed in the two solid phases (Phases I and II) of t-butylammonium tetrafluoroborate. Since the entropy change at the solid-solid phase transition is small compared with that ( $> R \ln 2$ ) expected for the transition accompanying a gain in orientational disorder of ions [16], and since no marked change in  $M_{2H}$ ,  $M_{2F}$ ,  $T_{1H}$ , or  $T_{1F}$  was observed, the crystal structure change here is considered to be so slight that the motional states of the cation and anion are little affected; probably only the correlation times of the motions in Phase II decrease to some extent at the transition.

- [1] H. Ishida, T. Iwachido, N. Hayama, R. Ikeda, M. Hashimoto, and D. Nakamura, *Z. Naturforsch.* **44a**, 71 (1989).
- [2] H. Ishida, T. Iwachido, N. Hayama, D. Nakamura, and R. Ikeda, *Bull. Chem. Soc. Jpn.* **64**, 3613 (1991).
- [3] Y. Kume, R. Ikeda, and D. Nakamura, *J. Magn. Reson.* **33**, 331 (1979).
- [4] H. Ishida, T. Iwachido, N. Hayama, R. Ikeda, M. Terashima, and D. Nakamura, *Z. Naturforsch.* **44a**, 741 (1989).
- [5] D. Pendred and R. E. Richards, *Trans. Faraday Soc.* **51**, 468 (1955).
- [6] A. P. Caron, D. J. Huettner, J. L. Ragle, L. Sherk, and T. R. Stengle, *J. Chem. Phys.* **47**, 2577 (1967).
- [7] K. N. Trueblood, *Acta Crystallogr.* **C43**, 711 (1987).
- [8] H. Ishida, S. Inada, N. Hayama, D. Nakamura, and R. Ikeda, *Ber. Bunsenges. Phys. Chem.* **95**, 866 (1991).
- [9] H. Ishida, T. Higashiyama, N. Hayama, and R. Ikeda, *Z. Naturforsch.* **47a**, 1087 (1992).
- [10] A. Abragam, *The Principles of Nuclear Magnetism*, Oxford University Press, London 1961.
- [11] D. E. O'Reilly, E. M. Peterson, and T. Tsang, *Phys. Rev.* **160**, 333 (1967).
- [12] S. Albert and H. S. Gutowsky, *J. Chem. Phys.* **59**, 3585 (1973).
- [13] H. Ishida, Y. Kubozono, S. Kashino, and R. Ikeda, *Z. Naturforsch.* **47a**, 1255 (1992).
- [14] M. B. Dunn and C. A. McDowell, *Mol. Phys.* **24**, 969 (1972).
- [15] H. Ishida, S. Inada, N. Hayama, D. Nakamura, and R. Ikeda, *Z. Naturforsch.* **46a**, 265 (1991).
- [16] N. G. Parsonage and L. A. K. Staveley, *Disorder in Crystals*, Clarendon Press, Oxford 1978.